

Influence of Vanadium Location in Titania Supported Vanadomolybdophosphoric Acid Catalysts and Its Effect on the Oxidation and Ammoxidation Functionalities

N. Lingaiah,* K. Mohan Reddy, P. Nagaraju, P. S. Sai Prasad, and Israel E. Wachs

Catalysis Laboratory, I&PC Division, Indian Institute of Chemical Technology, Hyderabad, 500 007 India, and Operando Molecular Spectroscopy & Catalysis Laboratory, Chemical Engineering Department, Lehigh University, Bethlehem, Pennsylvania 18015

Received: December 20, 2007; Revised Manuscript Received: March 7, 2008

Titania supported vanadomolybdophosphoric acid (VMPA) catalysts with vanadium in different positions, incorporated into the molybdophosphoric acid structure by substituting for molybdenum and cation exchanged on the molybdophosphoric acid surface, were synthesized. The catalysts were characterized by XRD, FT-IR, Raman spectroscopy, TPR, XPS, and ESR techniques. The FT-IR and Raman spectral analyses confirm that the molybdophosphoric acid is present with the Keggin ion structure during modifications. The incorporation of vanadium into the primary or secondary structures of the Keggin heteropoly acid was confirmed by ESR, Raman, and XPS analysis. These catalysts were investigated for the vapor phase ammoxidation of 2-methyl pyrazine and methanol oxidation. The specific location of vanadium in the 12-molybdophosphoric acid was found to affect the catalytic redox performance. The catalyst with vanadium present in the primary structure of the Keggin ion possesses enhanced catalytic redox activity and selectivity compared to when vanadium is present on the Keggin surface for both the ammoxidation and oxidation reactions.

1. Introduction

Heteropolyacids (HPAs) are negatively charged oxide clusters which mostly exist in the Keggin structures. HPAs are employed as both acid and oxidation catalysts for several industrial applications.^{1,2} The HPA compounds can be considered as molecular solids because of the finite number of atoms in such subnanometer sized clusters (e.g., the $H_3PMo_{12}O_{40}$ Keggin). The main advantage of HPAs is that their acidity and reactivity can be controlled by varying the addenda (Mo atoms in the above Keggin) or central atoms (e.g., P in the above Keggin) and the nature of the charge balancing cations (the protons in the above Keggin).³ The Keggin negative charge is balanced by protons or metal cations, which render the materials' acidic and redox properties. Cation exchange can also substitute the charge balancing protons via salt formation.⁴ These substituted cations also determine the crystallographic, secondary structure of the heteropoly compound. The additional cations in the secondary structure may also strongly affect the catalytic properties of the HPAs.^{5,6} It is also reported that one or more addenda atoms such as Mo or W can be substituted by another metal like vanadium.⁷ The addition of vanadium to a heteropoly compound improves its catalytic functionalities with respect to partial oxidations. The vanadium incorporated molybdophosphoric acid catalysts show unique catalytic features due to their bifunctional property, which arises due to the redox nature of vanadium and the acidic character of the molybdophosphoric acid.⁸ The molybdovanadophosphoric acid (VMPA) based catalysts are used commercially for the synthesis of methacrolein and in the conversion of isobutyric acid to methacrylic acid. The structural flexibility and redox capability of the vanadium centers is thought to facilitate an active participation of gas-phase molecular O_2 .⁹ Several authors have investigated VMPA catalysts by replacing 1–3 Mo atoms with the corresponding number of

V atoms.^{10,11} The main observation in the high vanadium incorporated systems is the expulsion of vanadium from the secondary structure and formation of a vanadyl (VO^{2+}) salt during catalysis.¹²

The objective of the present study is to examine the consequences of substituting vanadium atoms as addenda atoms for Mo or as charge balancing vanadyl cations for the protons in the $H_3PMo_{12}O_{40}$ Keggin. The incorporation of vanadium in the primary structure or as charge balancing protons is schematically shown¹³ in Figure 1. In addition, the effect of supporting the VMPA Keggin on TiO_2 was also investigated. Titania was chosen as a support because it preserves the Keggin unit to a higher temperature than its unsupported analogue. Moreover, deposition of heteropoly acid on solid supports is important for catalytic applications since the surface area of unsupported Keggin is low. Another important aspect of the titania support is that it is capable of releasing oxygen from the surface due to mobility of lattice oxygen and to form oxygen vacancies at relatively mild conditions.¹⁴ The supported VMPA/ TiO_2 catalysts were tested for ammoxidation of 2-methyl pyrazine and oxidation of methanol since the product distributions of these reactions are strongly influenced by their acid and redox characteristics. Ammoxidation of 2-methyl pyrazine (MP) to yield 2-cyano pyrazine (CP) is an important reaction as the CP is the precursor for the synthesis of pyrazinamide, an anti-TB drug.

2. Experimental

The 12-molybdophosphoric acid (MPA) was supplied by Loba Chemie, India, and the TiO_2 support (anatase) was obtained from Sigma Aldrich (24-857-6). Vanadium incorporated into the primary or secondary structure of MPA supported on titania catalysts was prepared by the impregnation method. Vanadium incorporated into the primary structure of the Keggin ion of molybdophosphoric acid on titania support was also prepared

* Author for correspondence. Phone: +91-40-27193163. Fax: +91-40-27160921. E-mail: nakkalingaiah@iict.res.in.

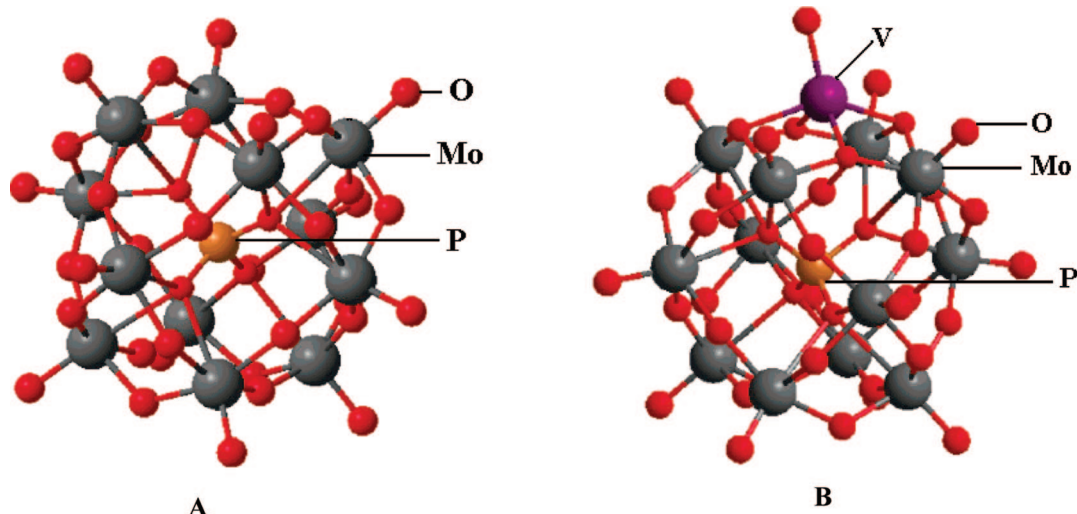


Figure 1. Structure (A) of the Keggin ion $[\text{PMo}_{11}\text{VO}_{40}]^{4-}$. One of the Mo's is replaced with V. Structure (B) of the Keggin ion $(\text{VO})[\text{PMo}_{11}\text{VO}_{40}]$, with $(\text{VO})^{2+}$ unit.

by the impregnation method. Prior to impregnation, the active masses with the vanadium incorporation into the primary structure of MPA were synthesized according to the procedure previously reported.^{15,16} In the synthesis of vanadium incorporated into the primary structure of MPA (i.e., $\text{H}_4\text{PMo}_{11}\text{V}_1\text{O}_{40}$ (VMPA)), hot aqueous solutions of disodium hydrogen phosphate and sodium metavanadate were mixed in the required proportions. The mixture was cooled and acidified with concentrated sulfuric acid. To this mixture an aqueous solution of sodium molybdate dihydrate was added. Concentrated sulfuric or hydrochloric acid was subsequently slowly added with stirring, and the color changed from dark red to light red. The VMPA formed was extracted with diethyl ether since the heteropoly acid was present in the middle layer as a heteropoly etherate. The ether was removed by passing air through the solution. The orange solid obtained was dissolved in water and concentrated until the crystals appeared.

In the case of vanadium in the secondary structure of MPA possessing the general formula $(\text{VO})\text{PMo}_{12}\text{O}_{40}$ (denoted as VOMPA), the VOMPA was first prepared by exchanging the protons with $(\text{VO})^{2+}$ ions. The required quantity of V_2O_5 was dissolved in oxalic acid at 100°C followed by cooling the solution to room temperature. This solution was added to the aqueous solution of MPA with constant stirring. The excess water was removed from the water bath, and the sample was dried at 120°C for 12 h.

Titania supported catalysts were prepared by adding a required amount of MPA, VMPA, and VOMPA in a minimum amount of water to support on titania. The excess solution was removed from the water bath, and the catalyst masses were dried in an air oven at 120°C for 12 h and calcined in air at 350°C for 4 h. These catalysts were denoted as MPA/ TiO_2 , VMPA/ TiO_2 , and VOMPA/ TiO_2 , respectively. In all the catalysts, 20 wt % active component (i.e., MPA, VMPA, VOMPA) was supported on the titania.

XRD patterns of the catalysts were recorded on a Siemens D-5000 diffractometer using $\text{Cu K}\alpha$ radiation. FTIR spectra were recorded on a Biorad-Excalibur series (USA) spectrometer using the KBr disk method. Temperature programmed reduction (TPR) of the catalysts was carried out in a flow of 10% H_2/Ar mixture gas at a flow rate of 30 mL/min with a temperature ramp of $10^\circ\text{C}/\text{min}$. Before the H_2 -TPR run, the catalysts were

pretreated with Argon gas at 250°C for 2 h. The hydrogen consumption was monitored using a thermal conductivity detector.

The Raman spectra of the samples were collected on a visible Raman spectrometer system (Horiba-Jobin Yvon LabRam-HR) equipped with a confocal microscope, 2400/900 grooves/mm gratings, and a notch filter. The visible laser excitation at 532 nm (visible/green) was supplied by a Yag doubled diode pumped laser (20 mW). The scattered photons were directed and focused onto a single-stage monochromator and measured with a UV-sensitive LN_2 -cooled CCD detector (Jobin Yvon CCD-3000V). The catalyst samples in powder form (about 5–10 mg) were usually loosely spread onto a glass slide below the confocal microscope for Raman measurements.

ESR spectra of the samples were recorded on a Bruker EMX-X band spectrometer at the X-band frequency 9.7667 GHz at 293 K. The spectra were calibrated with an ER 035 M NMR Gauss meter.

XPS measurements were conducted on a KRATOS AXIS 165 with a dual anode (Mg and Al) apparatus using Mg $\text{K}\alpha$ anode. The nonmonochromatized Al $\text{K}\alpha$ X-ray source ($h\nu = 1486.6$ eV) was operated at 12.5 kV and 16 mA. Before acquisition of the data, the sample was outgassed for about 3 h at 100°C under a vacuum of 1.0×10^{-7} torr to minimize surface contamination. The XPS instrument was calibrated using Au as standard. For energy calibration, the carbon 1s photoelectron line was used. The carbon 1s binding energy was taken as 285 eV. A charge neutralization of 2 eV was used to balance the charge up of the sample. The spectra were deconvoluted using a Sun Solaris based Vision-2 curve resolver. The location and the full width at half-maximum (fwhm) value for the species were first determined using the spectrum of the pure sample. Symmetric Gaussian shapes were used in all cases.

Elemental analysis of the heteropoly acid samples was estimated by inductively coupled plasma atomic emission spectroscopy (ICP-MAS). The samples were digested using aquaregia, and the elements to be analyzed are phosphorus, molybdenum, and vanadium.

Amoxidation of 2-methyl pyrazine (MP) was carried out in a microreactor at atmospheric pressure in the temperature range of 360 to 420°C . In a typical experiment, about 5 g of the catalyst (crushed to 18/25 BSS sieve to eliminate mass transfer limitation and diluted with an equal quantity of quartz

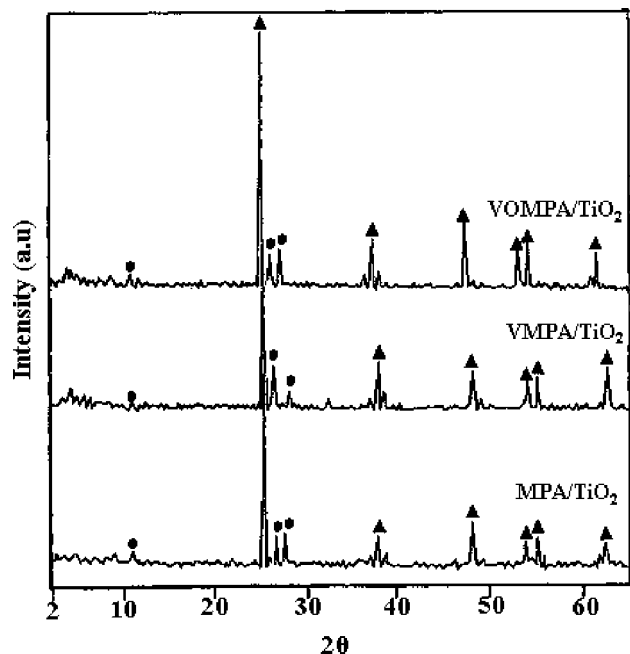


Figure 2. X-ray diffraction patterns of the catalysts under ambient conditions: (●) Keggin ion; (▲) TiO_2 .

beads) was loaded in the reactor suspending it between two quartz plugs. The feed with a molar ratio of MP/water/ammonia/air = 1:13:7:38 was fed into the preheated portion of the reactor. The aqueous mixture of MP was metered using a microprocessor-based feed pump (B. Braun, Germany), at a flow rate of 2 mL/h. After allowing the catalyst to attain steady state for 30 min, at each reaction temperature, the liquid product was collected for 30 min, and it was analyzed by gas chromatography, separating it on an OV-101 column (2 m long, 3 mm diameter) using an FID detector.

Methanol oxidation was carried out in a fixed-bed catalytic microreactor using about 50 mg of catalyst with a total gas flow rate of $100 \text{ cm}^3 \text{ (NTP) min}^{-1}$. The molar feed gas composition in the methanol/oxygen/helium stream was 6:13:81, respectively. The products were analyzed with an online gas chromatograph (HP 5840) equipped with both TCD and FID detectors and using two columns: a capillary column (CP-sil 5CB) for methylal, dimethyl ether, and methyl formate analysis and a packed column (Carboxene-1000) for methanol and formaldehyde analysis.

3. Results and Discussion

The XRD patterns of the titania supported MPA, VMPA, and VOMPA catalysts are presented in Figure 2. The XRD patterns are dominated by the peaks of the crystalline anatase phase of TiO_2 support. Only small diffraction lines from the supported Keggin ions are present in Figure 2 indicated by circles. The elemental analysis of these catalysts was estimated by ICP-MAS. Keggin units have one central atom, 12 transition metal atoms, and an appropriate number of charge balancing protons or cations. The Mo/P ratio of the standard (ideal formula $\text{H}_3\text{PMo}_{12}\text{O}_{40}$) was 12.6, indicating a relatively pure phase of the heteropolyacid. The Mo/P ratios in our synthesized pure VMPA and VOMPA samples were 11.1 and 12.3, respectively. The pure VMPA catalyst consists of slightly lower contents of Mo in the Keggin units due to partial substitution of Mo by the other cation. Indeed, the V/P ratio in this sample is 0.92. The Mo/P ratios for supported catalysts, MPA/TiO_2 , VMPA/TiO_2 ,

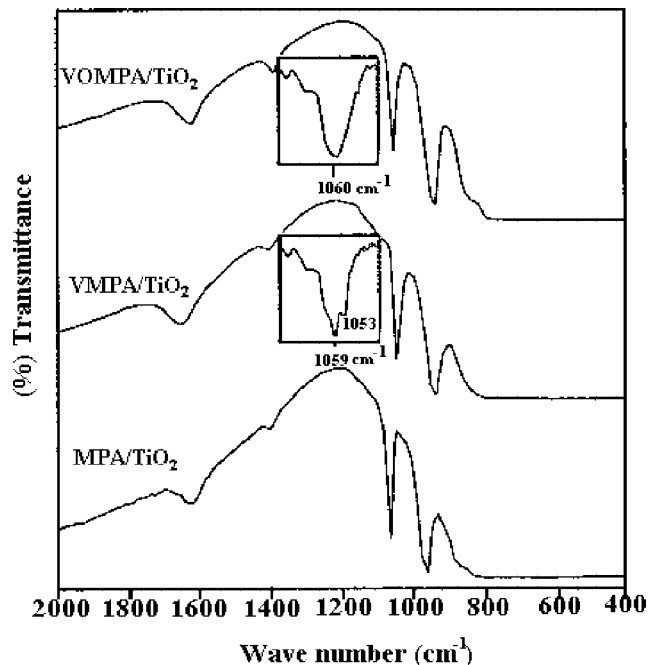


Figure 3. FT-IR spectra of the catalysts under ambient conditions.

and VOMPA/TiO_2 , were 12.1, 10.8, and 11.9, respectively. Since elemental analysis of the bulk solids cannot provide information on the phases present in the solid, we used a variety of techniques including FT-IR and Raman vibrational analysis to obtain additional structural insights into the nature of the supported Keggin ions.

The FT-IR spectra of the titania supported catalysts are presented in Figure 3. The catalysts mainly exhibit bands at 1063, 963, and 860 that are assigned to stretching vibrations of P-O_a (O_a = oxygen atoms bound to three Mo atoms and to P), Mo-O_t (O_t = terminal oxygen atom), and $\text{Mo-O}_b\text{-Mo}$ (O_b = corner sharing bridging oxygen atom), respectively.¹⁷ The TiO_2 support absorbs the IR signal below 800 cm^{-1} that prevents collection of weak Keggin vibrations in this region. To confirm that vanadium was incorporated into the MPA Keggin ion, FTIR analysis was conducted prior to supporting VMPA and VOMPA on the titania support.

With a V atom substituting for Mo in the primary structure of the oxoanion (pure VMPA catalyst), the P-O and Mo=O bands shifted toward lower wavenumbers ($\approx 5 \text{ cm}^{-1}$) due to a reduced structure symmetry.¹⁶ This is an interesting observation compared with pure MPA catalyst. No changes were observed for pure VOMPA catalyst apart from an appearance of a shoulder near 1000 cm^{-1} that is due to the presence of VO^{2+} as counterions.¹⁸ The FTIR spectra of the titania supported catalysts are well conserved with Keggin structure. Compared to their pure catalysts, VMPA/TiO_2 and VOMPA/TiO_2 showed a marginal shift in the Keggin ion vibrations ($\leq 3 \text{ cm}^{-1}$). For the VMPA/TiO_2 catalyst, a shoulder was observed at 1053 cm^{-1} , along with a P-O_a stretching vibration at 1059 cm^{-1} . The VOMPA/TiO_2 catalyst showed a broad band in this region, indicating the presence of counterions. It is known that the introduction of a metal other than Mo in the Keggin ion induces a decrease in the Mo-O_t stretching frequency with a possible splitting of the P-O_a band.¹⁹ This splitting suggests the incorporation of V into the primary structure of the Keggin ion. The FT-IR data suggest the retention of the Keggin structure during the impregnation of heteropoly acid on titania support.

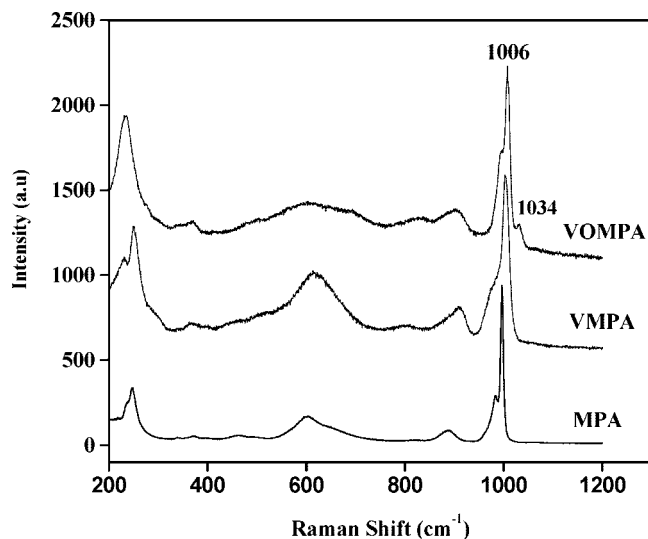


Figure 4. Raman spectra of the unsupported heteropoly acid catalysts.

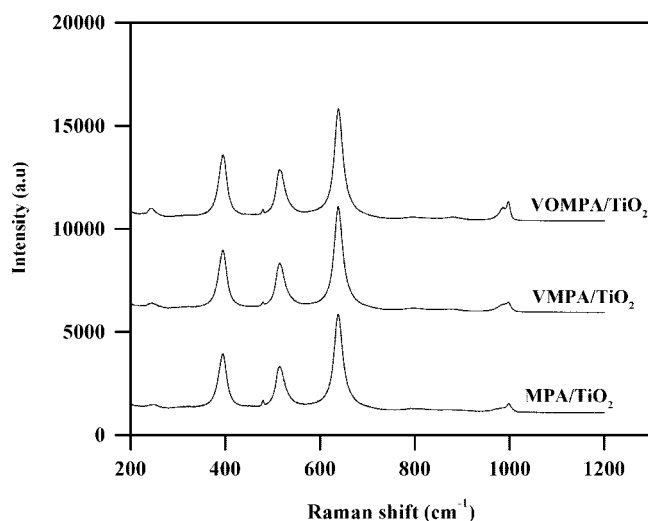


Figure 5. Raman spectra of the titania supported heteropoly acid catalysts.

The Raman spectra of the pure MPA, VMPA, and VOMPA catalysts are presented in Figure 4. The pure MPA, VMPA, and VOMPA catalysts possess bands at 1006, 990, 900, 600, and 242 cm^{-1} . These Raman bands are ascribed due to Keggin ion vibrations. The pure VOMPA Keggin contains an additional band at 1034 cm^{-1} .²⁰ The bands at 1006 and 990 cm^{-1} arise from the stretching vibrational modes of the $\text{Mo}=\text{O}_t$ bond.²¹ The Raman bands around 900 and 600 cm^{-1} are associated with the asymmetric stretching vibrational mode of the bridging $\text{Mo}-\text{O}_b-\text{Mo}$ and the bending mode of $\text{O}-\text{P}-\text{O}$ bonds, respectively.²² The band at 242 cm^{-1} originates from the bridging $\text{Mo}-\text{O}-\text{Mo}$ bending mode of the intact Keggin structure.¹² The additional band at 1034 cm^{-1} for the pure VOMPA Keggin is characteristic of the $\text{V}=\text{O}_t$ bond of the surface vanadyl cation.²³

The Raman spectra of the supported MPA, VMPA, and VOMPA are presented in Figure 5 in the 200–1200 cm^{-1} region. The Raman spectral features below the 900 cm^{-1} vibrational region are dominated by the crystalline TiO_2 (anatase) spectrum. The Raman spectra exhibit vibrations at 1006 and 990 cm^{-1} characteristic of $\text{Mo}=\text{O}_t$ symmetric and asymmetric stretching vibrations²⁴ that demonstrate the Keggin ions are intact on the TiO_2 support after impregnation.

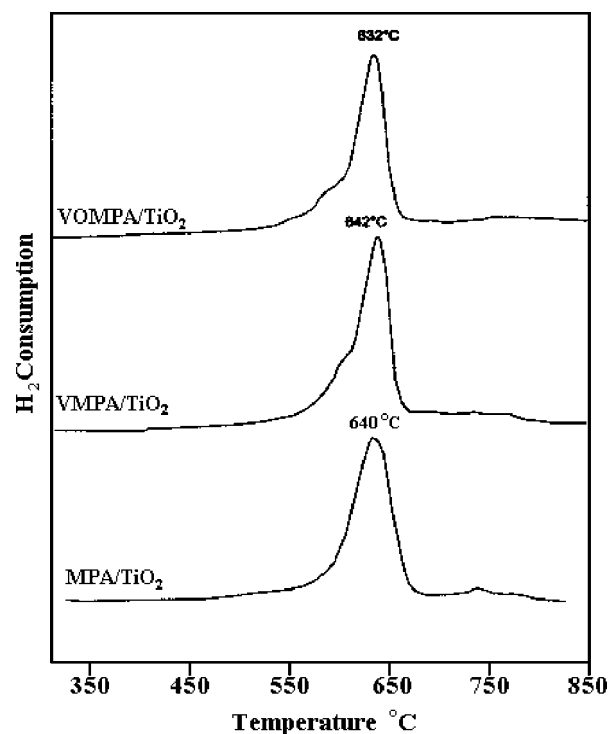


Figure 6. Temperature programmed reduction profiles of the catalysts.

The H_2 -TPR patterns of the supported MPA/TiO_2 , VMPA/TiO_2 , and (VO) MPA/TiO_2 catalysts are exhibited in Figure 6. All the samples show one main reduction peak centered at ≈ 640 $^\circ\text{C}$. As the heteropoly acids generally decompose above 500 $^\circ\text{C}$, the reduction peaks are ascribed to the reduction of free metal oxides formed by the decomposition of the Keggin ion during the H_2 -TPR experiment. The H_2 -TPR spectra of the titania supported Keggin catalysts with vanadium in the primary or secondary structure are different from that of the MPA/TiO_2 catalyst. A small reduction peak is observed below 640 $^\circ\text{C}$ in the case of VMPA/TiO_2 and (VO) MPA/TiO_2 catalysts, which can be attributed to the reduction of segregated vanadium oxide entities.²⁵ The incorporation of V centers in the Keggin ion does not cause a pronounced destabilization of the Keggin units. Vanadium centers are quite stable in the lacunary Keggin ion of V_x [$\text{PVMo}_{11-x}\text{O}_{40}$] that forms under reaction conditions. It should be noted that the reduction temperature for vanadium oxide entities in the (VO) MPA/TiO_2 catalyst is slightly less compared to the VMPA/TiO_2 catalyst. This is an interesting observation made by TPR indicating that V located in the Keggin unit (primary structure) is more stable compared to V located at the cationic position (secondary structure). Moreover, V centers can change their oxidation state from V^{5+} to V^{4+} without a significant detectable destabilization of the lacunary Keggin ion.⁹

ESR is an important technique to investigate the $\text{V}^{4+}/\text{V}^{5+}$ species in the catalysts. The room-temperature ESR spectra of VMPA/TiO_2 and $\text{VOMPA}/\text{TiO}_2$ calcined samples are shown in Figure 7. The VOMPA catalyst gave a spectrum nearly identical to the spectrum of $\text{H}[\text{VO}(\text{H}_2\text{O})_5][\text{PMo}_{12}\text{O}_{40}] \cdot 8\text{H}_2\text{O}$ indicating the presence of V^{4+} species and their environment should be identical in these two cases.^{26,27} The VOMPA spectrum is characteristic of an unpaired 3d electron ($S = 1/2$) interacting with the nuclear spin ($I = 7/2$) of a V^{4+} ion. The spectrum exhibits eight broad parallel and perpendicular lines showing that the V^{4+} ion in a tetragonal ligand field with $g^{\parallel} =$

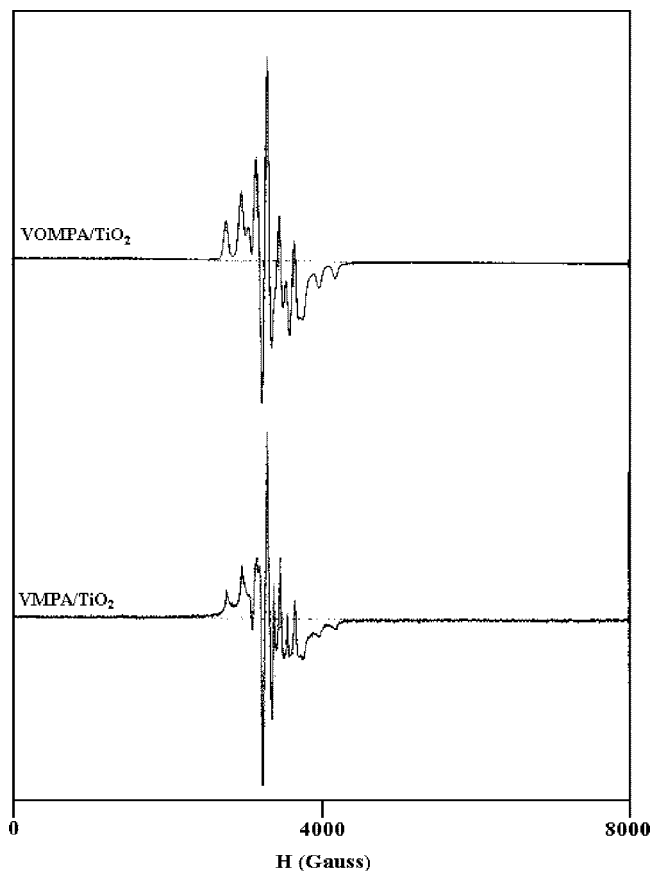


Figure 7. ESR spectra of VOMPA/TiO₂ and VMPA/TiO₂ catalysts.

TABLE 1: Binding Energies of Core Electron Levels and XPS Atomic Ratios for Titania Supported Heteropoly Compounds

catalyst	binding energy (eV)					Mo/Ti ratios
	P 2p	O 1s	Mo 3d _{5/2}	V 2p _{3/2}	Ti 2P	
MPA/TiO ₂	134.2	531.6 532.2	233.4	—	459.5	0.55
VMPA/TiO ₂	133.8	531.4 532.5	232.9	517.6	459.4	0.37
VOMPA/TiO ₂	133.6	531.2 532.6	232.6	516.2	459.6	0.33

1.925, $g^{\perp} = 1.976$, $A^{\parallel} = 204$ G, and $A^{\perp} = 98$ G. This signal has been found in the case of $H[VO(H_2O)_5][PMo_{12}O_{40}]$ corresponding to isolated V^{4+} surrounded by one terminal oxygen and five water molecules as ligands. These $[VO(H_2O)_5]^{+2}$ ions are known to be located in a cation position outside the Keggin units. Due to the similarity of the spin Hamiltonian parameters with the previously reported values,²⁸ one can assign the ESR signal in the VOMPA catalyst as being related to VO^{+2} sites outside the Keggin units. The EPR spectrum of VMPA catalysts shows the characteristic signal for V^{+5} species with hyperfine structure as reported by Bruckner et al.²⁰ The spin Hamiltonian parameters for this catalyst are $g^{\parallel} = 1.934$, $g^{\perp} = 1.972$, $A^{\parallel} = 163$ G, and $A^{\perp} = 54$ G. This agrees with the location of V^{+5} in the octahedral sites of intact Keggin units. Thus, the ESR data clearly show the location of V in the catalysts, and these results are in accordance with XRD and IR results.

The binding energies (BEs) of various core-electron levels (O 1s, P 2p, Ti 2p, V 2p_{3/2}, and Mo 3d_{5/2}) for supported heteropoly compounds are summarized in Table 1. The BEs for the P 2p core level for all samples are in the region of 133.6–134.2 eV. The BE values of P 2p confirm that phos-

phorus is a phosphate.²⁹ The BEs for the Ti 2p core level are observed at 459.5 ± 0.1 eV for all the supported catalysts, suggesting that the oxidation state of titanium is Ti^{4+} .³⁰ Two well-defined peaks of the O 1s core level were noticed at 531.6 and 532.2 eV for these catalysts. The first peak is attributed to oxygen of TiO₂ support, and the latter one is due to Mo–O–Mo, Mo–O–P, and/or Mo–O–H in polymolybdate structures.³¹ The BE values for the Mo 3d_{5/2} core level at 232.6 ± 1 eV for these samples suggest the presence of Mo^{6+} ions in polymolybdates.²⁹

The BE of the V 2p_{3/2} core level for VMPA/TiO₂ at 517.6 eV is characteristic of V^{5+} ions.³² A decrease in the BE of V 2p_{3/2} for VOMPA/TiO₂ at 516.2 indicates the presence of the V^{4+} ion. In addition, the broadening of the V 2p_{3/2} peak for this catalyst can be attributed to the presence of surface vanadium with different valence state. The V-substituted MPA catalysts showed lower XPS Mo/Ti ratios compared to that of MPA/TiO₂. Predoeva et al.³³ have also observed the decrease in the Mo/Ti ratios for titania supported vanadium containing heteropoly acids. The XPS results are in accordance with ESR data and suggest the presence of lower vanadium oxidation species in VOMPA/TiO₂ catalyst.

The MPA catalysts with and without vanadium were investigated for their catalytic activity for the ammoxidation of MP. The MP ammoxidation catalytic activity expressed in terms of yield at a reaction temperature of 380 °C is shown in Figure 8. The Keggin catalyst with incorporated vanadium in the primary structure shows higher yield to CP than the vanadium-free MPA catalyst. Incorporation of vanadium into the primary Keggin structure results in a much higher yield than the Keggin with exchanged vanadium on the surface (VOMPA). The difference in the catalytic behavior of the catalysts can be attributed to the difference in the location of the vanadium atom in the heteropoly acid. It has been reported that substitution of V^{5+} for Mo^{6+} in the HPAs results in the generation of more reactive lattice oxygen associated with the Mo–O–V species.²⁴ Oxidation reactions catalyzed by vanadium occur by a redox reaction normally followed by the Mars–Van Krevelen mechanism that employs lattice oxygen for the oxidation of the organic substrate, and the gas phase oxygen supplements the loss of lattice oxygen. The lattice oxygen also plays an important role in the oxidation and reduction cycle of V during the ammoxidation reaction by enhancing its reactivity. The difference in functionality of vanadium atoms in heteropoly compounds arises due to the very different susceptibility of vanadyl cations and vanadium atoms in the Keggin structure for reoxidation process.³⁴ Garte et al. reported that the vanadium atoms present in the Keggin

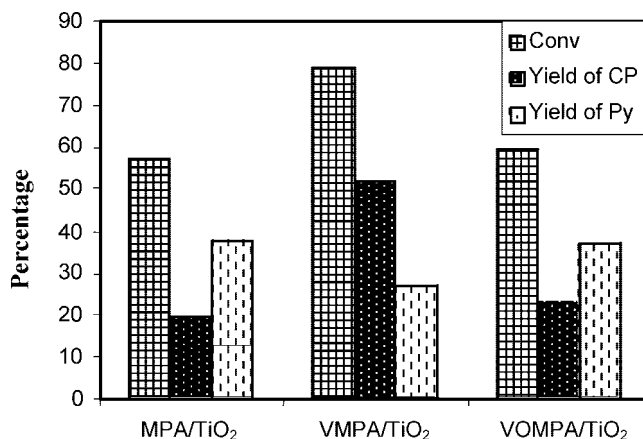


Figure 8. Catalytic activity of the supported heteropoly acid catalysts in MP ammoxidation at 380 °C.

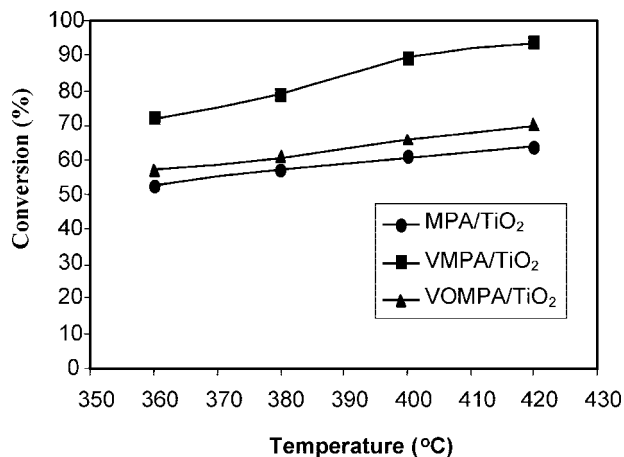


Figure 9. Effect of reaction temperature on the conversion in ammoxidation of MP over titania supported heteropoly acid catalysts.

structure, when reduced to V^{4+} , are easily reoxidized, while the reoxidation of $(VO)^{2+}$ vanadyl ions occurs at a much slower rate even at higher temperature.³⁵ In the ammoxidation reaction, the catalyst activity mainly depends upon how rapidly the catalyst undergoes the oxidation–reduction cycle. Thus, it is for this reason that the VMPA/TiO₂ catalyst exhibits higher activity than the VOMPA/TiO₂ catalyst for the ammoxidation reaction. The effect of reaction temperature is carried out over these catalysts, and the results are presented in Figure 9. The activity of the catalysts are in the following order at any given temperature: VMPA/TiO₂ > (VO)MPA/TiO₂ > MPA/TiO₂. It shows that at any reaction temperature the MPA/TiO₂ catalyst exhibits high conversion, and the conversion increased with an increase in reaction temperature. These results suggest that the presence of vanadium in the primary structure leads to an increase in the selectivity of the desired product as well as the overall activity. It observed an increase in rate by one and a half times and about a 3-fold increase in selectivity for the vanadium-containing catalyst compared with the catalyst without vanadium in the primary structure of the Keggin ion.

The redox characteristics of the supported MPA, VMPA, and VOMPA catalysts were further probed by methanol oxidation. Methanol is a “smart” chemical probe molecule that provides information about the nature of redox, acidic, and basic sites by forming HCHO, CH₃OCH₃ (DME), and CO/CO₂, respectively, as reaction products. The CH₃OH conversion and product selectivity over the supported VMPA and VOMPA catalysts are listed in Table 2. The supported VMPA catalyst exhibits a much higher methanol conversion and HCHO selectivity than the supported MPA and VOMPA catalysts, which reflects the redox behavior of this catalyst. The supported MPA catalyst is selective to DME and exhibited selectivity to HCHO only at high reaction temperature. Note that the supported MPA and VOMPA catalysts only yield DME from acidic sites at lower reaction temperatures, which reflects the absence of redox characteristics at the lower reaction temperatures. Only at 300 °C does the redox pathway of CH₃OH oxidation to HCHO over the supported VOMPA catalyst open up. In this reaction, negligible quantities of CO/CO₂ were formed as a byproduct. Apart from the location of vanadium in the Keggin structure, the number of vanadium atoms per Keggin unit is also important. The few reports about methanol oxidation over the vanadium containing molybdenum-based heteropoly acids found that the HCHO selectivity increases with incorporation of vanadium into MPA with maximum selectivity attained with two vanadium

TABLE 2: CH₃OH Oxidation over TiO₂ Supported Heteropoly Acids^a

catalyst	reaction temperature (°C)	activity (mol/g/h)	selectivity			
			HCHO	DME	MF	DMM
MPA/TiO ₂	250	1.06	--	100	--	--
	275	2.46	--	100	--	--
	300	4.18	16	81	2	1
VMPA/TiO ₂	250	6.27	23	74	2	1
	275	7.37	21	76	2	1
	300	13.09	36	59	4	1
VOMPA/TiO ₂	250	1.58	--	100	--	--
	275	3.03	--	100	--	--
	300	6.2	30	67	2	1

^a DME, dimethyl ether; MF, methyl formate; DMM, dimethoxy methane.

atoms.^{36,37} It is also reported that in the case of molybdenum-based heteropoly acids substitution with more vanadium causes a decrease in activity with an increase in vanadium content.³⁸ It has been rationalized that the HPA Keggin structure can only tolerate one vanadium per Keggin unit since higher vanadium content destabilizes the crystalline molecular structure.³⁹

4. Conclusions

Vanadium incorporated into the primary (VMPA) or secondary (VOMPA) structures of 12-molybdophosphoric acid catalysts was synthesized and investigated for the vapor phase ammoxidation of 2-methyl pyrazine and methanol oxidation. FT-IR and Raman analyses under ambient conditions indicate the location of vanadium in these catalysts. The vanadium present in the primary Keggin structure leads to high catalytic activity and selectivity during 2-methyl pyrazine ammoxidation to 2-cyano pyrazine. This catalyst is also more active and selective toward the formation of formaldehyde during methanol oxidation. The extent of oxidation–reduction during these oxidation reactions is thought to be responsible for the higher activity of the VMPA than the VOMPA catalyst during these oxidation reactions. The oxidation and ammoxidation results suggest that the location of vanadium plays an important role in activity and selectivity.

Acknowledgment. N. Lingaiah thanks the Department of Science & Technology, New Delhi, India, for the financial assistance in the form of the BOYSCAST fellowship.

References and Notes

- (1) Okuhara, T.; Mizuno, N.; Misono, M. *Adv. Catal.* **1996**, *41*, 1131.
- (2) Cavani, F.; Trifiro, F. *Catal. Today* **1999**, *51*, 561.
- (3) Misono, M. *J. Chem. Soc., Chem. Commun.* **2001**, *11*, 41.
- (4) Mizuno, N.; Han, W.; Kudo, T. *J. Catal.* **1998**, *178*, 391.
- (5) Bardin, B. B.; Davis, R. J. *Appl. Catal., A* **1999**, *185*, 283.
- (6) Cavani, F.; Tanguy, A.; Trifiro, F.; Koutyrev, M. *J. Catal.* **1998**, *174*, 231.
- (7) Bruckman, K.; Tatibouet, J. M.; Che, M.; Serwicka, E.; Haber, J. *J. Catal.* **1993**, *139*, 455.
- (8) Kozhevnikov, I. V. *J. Mol. Catal. A* **1997**, *111*, 109.
- (9) Ressler, T.; Timpe, O.; Girgsdies, F.; Wienold, J.; Neisius, T. *J. Catal.* **2005**, *231*, 279.
- (10) Liu, H.; Iglesia, E. *J. Phys. Chem. B* **2003**, *107*, 10840.
- (11) Liu, H.; Iglesia, E. *J. Catal.* **2004**, *223*, 161.
- (12) Mestl, G.; Ilkenhans, T.; Spielbaur, D.; Dieterle, M.; Timpe, O.; Krohnert, J.; Jentoft, F.; Knozinger, H.; Schlögl, R. *Appl. Catal., A* **2001**, *210*, 13.
- (13) Gutjahr, M.; Hoentsch, J.; Böttcher, R.; Storcheva, O.; Köhler, K.; Pöppel, A. *J. Am. Chem. Soc.* **2004**, *126*, 2905.
- (14) Herrmann, J. M.; Disdier, J. *Catal. Today* **2000**, *56*, 389.
- (15) Tsigdinos, G. A.; Hallada, C. J. *Inorg. Chem.* **1968**, *7*, 437.
- (16) Casarini, D.; Centi, G.; Jiru, P.; Lena, V.; Tvaruzkova, Z. *J. Catal.* **1993**, *143*, 325.

- (17) Bondareva, V. M.; Andrashkevich, T. V.; Detusheva, L. G.; Litvak, G. S. *Catal. Lett.* **1996**, *42*, 113.
- (18) Liu-Caia, F. X.; Phamb, C.; Beya, F.; Hervéa, G. *React. Kinet. Catal. Lett.* **2002**, *75*, 305.
- (19) Rocchiccioli-Deltcheff, C.; Fournier, M. *J. Chem. Soc., Faraday Trans.* **1991**, *87*, 3913.
- (20) Bruckner, A.; Scholz, G.; Heidmann, D.; Schneider, M.; Herein, D.; Bentrup, U.; Kant, M. *J. Catal.* **2007**, *245*, 369.
- (21) Busca, G. *J. Raman Spectrosc.* **2002**, *33*, 348.
- (22) Rocchiccioli-Deltcheff, C.; Aouissi, A.; Bettahar, M. M.; Launay, S.; Fournier, M. *J. Catal.* **1996**, *164*, 16.
- (23) Caliman, E.; Dias, J. A.; Dias, S. C. L.; Prado, A. G. S. *Catal. Today* **2000**, *107/108*, 816.
- (24) Hardcastle, F. D.; Wachs, I. E. *J. Phys. Chem.* **1991**, *95*, 5031.
- (25) Li, X.; Zhao, J.; Ji, W.; Zhang, Z.; Chen, Y.; Au, C.; Han, S.; Hibst, H. *J. Catal.* **2005**, *237*, 58.
- (26) Okuhara, T.; Kimura, M.; Kawai, T.; Xu, Z.; Nakato, T. *Catal. Today* **1998**, *45*, 73.
- (27) Lee, J. K.; Russo, V.; Melsheimer, J.; Köhler, K.; Schlögl, R. *Phys. Chem. Chem. Phys.* **2000**, *2*, 2977.
- (28) Bayer, R.; Marchal, C.; Liu, F. X.; Teze, A.; Herve, G. *J. Mol. Catal. A.* **1996**, *110*, 65.
- (29) Wang, E. B.; Shan, Y. K.; Liu, Z. X.; Zhang, B. *J. Acta Chim. Sin.* **1991**, *49*, 774.
- (30) Damyanova, S.; Fierro, J. *Chem. Mater.* **1998**, *10*, 871.
- (31) Jalil, P. A.; Faiz, M.; Tabet, N. M.; Hamdan, N.; Hussain, Z. *J. Catal.* **2003**, *217*, 292.
- (32) Delichere, P.; Bere, K. E.; Abon, M. *Appl. Catal., A* **1998**, *172*, 295.
- (33) Predoeva, A.; Damyanova, S.; Gaigneaux, E. M.; Petrov, L. *Appl. Catal., A* **2007**, *319*, 14.
- (34) Sopa, M.; Waclaw-Held, A.; Grossy, M.; Pijanka, J.; Nowinska, K. *Appl. Catal., A* **2005**, *285*, 119.
- (35) Garte, J. H.; Hamm, D. R.; Mahajan, S. In *Polyoxometalates: From Platonic Solids to Anti-Retroviral Activity*; Pope, M. T., Muller, A., Eds.; Kluwer Academic Publisher: Norwell, MA, 1994; p 281.
- (36) Liu, H.; Iglesia, E. *J. Phys. Chem. B* **2003**, *107*, 10840.
- (37) Liu, H.; Iglesia, E. *J. Catal.* **2004**, *223*, 161.
- (38) Bruckman, K.; Tatibouet, J.-M.; Che, M.; Serwicka, E.; Haber, J. *J. Catal.* **1993**, *139*, 455.
- (39) Watzenberger, O.; Emig, G.; Lynch, D. T. *J. Catal.* **1990**, *124*, 247.

JP7119476